

Model Predictive Pulse Pattern Control of Medium-Voltage Neutral-Point-Clamped Inverter Drives

Tobias Geyer, *Senior Member, IEEE*, Vedrana Spudić, *Member, IEEE*,
Wim van der Merwe, *Senior Member, IEEE*, and Ester Guidi, *Member, IEEE*

Abstract—Model predictive pulse pattern control (MP³C) combines the dynamic performance of direct torque control with the superb harmonic performance of optimized pulse patterns during steady-state operation. In doing so, MP³C maximizes the effectiveness of variable speed drive systems by fully utilizing the capability of the power electronic hardware and the electrical machine. Experimental results for a medium-voltage neutral-point-clamped inverter driving a 3.3 kV induction machine rated at 1140 kVA are reported, and the customer benefits of MP³C are discussed in detail.

I. INTRODUCTION

Medium-voltage (MV) drive systems are widely used in industry to lower the energy consumption of industrial processes [1]. In pump or fan applications, it is beneficial to use variable speed drives rather than mechanical throttling. The energy savings in MV systems, due to the high installed power, is large.

However, the energy efficiency brought about by the drive system is in many applications only a small part of the overall customer benefit. Specifically, the variable speed drive offers precise and accurate control of the system process. This is paramount for hot and cold rolling metal mills, for which the quality of the finished product depends largely on the precise control of the rolls' rotational speed. Controlling the speed is particularly demanding, because the material enters and leaves the rolls abruptly; as a result, the mechanical load on the rolls jumps between no load and full load frequently.

Fast control is also important in other applications, such as marine propulsion. During network disturbances, particularly when the supply voltage recovers, the control system must quickly and accurately react to maintain the dc-link voltage at an adequate level to avoid trips of the drive system. This is particularly important during harbor entrance navigation, which requires a high degree of reliability and availability of the propulsion system.

The strong focus on drive system efficiency and the necessity of fast acting, accurate and robust control of the process place unique demands on the control and modulation methods used in MV drives. To increase the efficiency, the number of

switching events per fundamental cycle is kept at a minimum. The energy stored in the dc-link capacitors is typically reduced to a minimum to increase safety in the event of MV faults. The control system must adhere to these boundary conditions while providing superior robustness and fast response times.

II. CONTROL METHODS FOR MV DRIVES

Several control methodologies have been developed for MV drives. A notable example is direct torque control (DTC), which controls the electromagnetic torque and the magnetization of the electrical machine using hysteresis controllers and a switching table [2]. DTC is renowned for its fast and precise torque steps, and it is generally considered to maximize the dynamic performance of a drive system. Furthermore, the hysteresis controllers and the lack of any rotor information make DTC extremely robust to dc-link voltage fluctuations and other system imperfections. As a result, DTC is commonly used in MV drives. However, the harmonic performance, in particular the current distortions for a given switching frequency, tend to be pronounced, as indicated in Fig. 1.

A widely used alternative to DTC is field-oriented control (FOC) [3], [4], which is formulated in a rotating orthogonal reference frame. Linear current controllers provide modulating

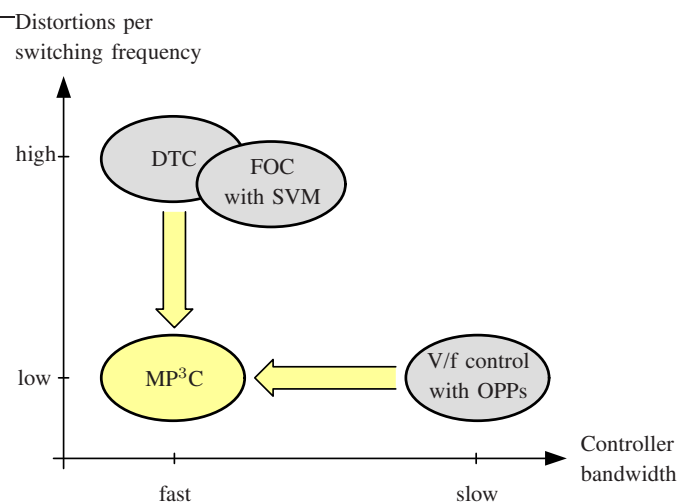


Fig. 1: Model predictive pulse pattern control (MP³C) combines the merits of direct torque control (DTC) during transients with those of optimized pulse patterns (OPPs) during steady-state operation

T. Geyer and V. Spudić are with ABB Corporate Research, Baden-Dättwil, Switzerland; e-mail: t.geyer@ieee.org, vedrana.spudic@ch.abb.com

W. van der Merwe and E. Guidi are with ABB Medium-Voltage Drives, Turgi, Switzerland; e-mail: wim.van-der-merwe@ch.abb.com, ester.guidi@ch.abb.com

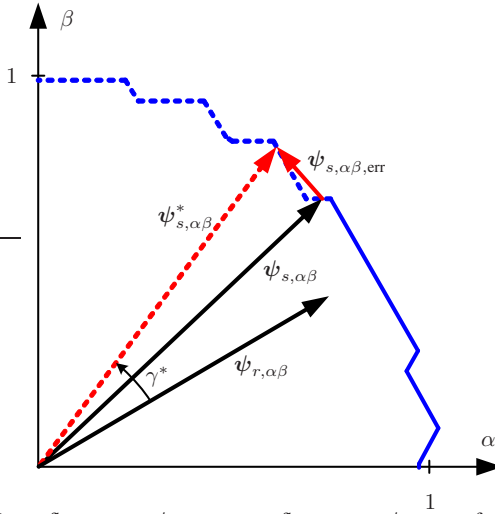


Fig. 2: Rotor flux vector $\psi_{r,\alpha\beta}$, stator flux vector $\psi_{s,\alpha\beta}$, reference stator flux vector $\psi_{s,\alpha\beta}^*$ and stator flux error $\psi_{s,\alpha\beta, err}$ in stationary coordinates

signals to a subsequent modulator, which is typically based on carrier-based pulse width modulation (CB-PWM) or space vector modulation (SVM). Because high-power MV converters operate at low switching frequencies in the range of a few hundred Hertz, the ratio between the switching frequency and the fundamental frequency, the so-called pulse number, is typically below 10. At such low pulse numbers, SVM exhibits high harmonic distortions for a given switching frequency, as shown in Fig. 1. The dynamic performance of FOC tends to be worse than that of DTC.

Optimized pulse patterns (OPPs) allow the minimization of the current distortions for a given switching frequency [5]. Conceptually, OPPs are a particularly attractive choice for MV converter systems. Traditionally, however, it has only been possible to use OPPs in a modulator driven by a very slow control loop, such as volts per frequency (V/f) control, see Fig. 1. When the operating point changes or when transitions between different pulse patterns occur, the absence of a fast controller leads to a poor dynamic performance and to large deviations of the currents from their references. This makes V/f control of OPPs ill-suited for MV drives application that require fast dynamics.

Squaring the circle, model predictive pulse pattern control (MP³C) [6] combines the dynamic performance of high-bandwidth controllers such as DTC with the superb harmonic performance of OPPs during steady-state operation. More specifically, MP³C achieves a nearly optimum ratio of harmonic current distortions per switching frequency at steady-state. During transients, very short current and torque responses are achieved that are similar to those of DTC, provided that additional pulses may be inserted when required [7].

MP³C combines the modulator and inner (current) control loop in one computational stage using the notion of model predictive control (MPC) [8]. For a given input trajectory, an internal model of the drive system predicts the system's output trajectory over a prediction horizon, a cost function

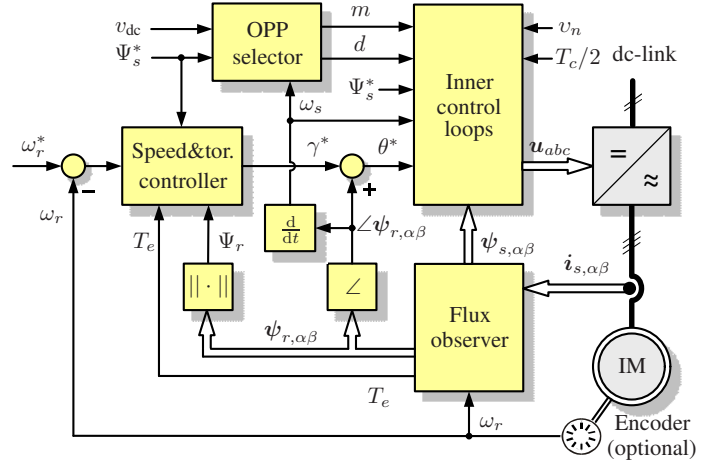


Fig. 3: Outer control loops of MP³C

maps these input and output trajectories into a scalar cost value, an optimization stage minimizes the cost function and computes the optimal control input, and the receding horizon policy provides feedback and robustness [9].

Compared to earlier flux trajectory controllers [10], [11], MP³C requires only the instantaneous stator flux vector, rather than its fundamental and ripple components. This greatly simplifies the flux observer design. The sampling frequency is 20 times higher, enabling a high controller bandwidth. The receding horizon policy provides robustness to parameter uncertainties and flux observer noise. Noteworthy extensions of the trajectory control principle have been developed, such as the optional insertion of additional switching transitions to shorten torque transients [7], the online generation of CB-PWM pulse patterns to extend MP³C seamlessly to low-speed operation [12], and the balancing of the neutral point (NP) potential to address neutral-point-clamped (NPC) converters.

MP³C is equally applicable to machine-side inverters and grid-side converters, including variable speed drives with induction and synchronous machines, and active rectifier units. MP³C has also been applied to modular multilevel converters used as STATCOMs [13] and railway grid interties [14]. To this end, MP³C was extended to address the balancing of a neutral point potential, the control of flying capacitor voltages [15], the active damping of filter resonances [16] and the control of circulating currents in modular multilevel converters [13], [14].

III. MODEL PREDICTIVE PULSE PATTERN CONTROL

Starting with the initial version in [17], the MP³C control method has been extended and revised during the past few years. The established controller framework is summarized in this section.

A. Offline Computation

OPPs are computed in an offline procedure by calculating the optimal switching angles and switching transitions. Typically, the aim is to minimize the current distortions for a given

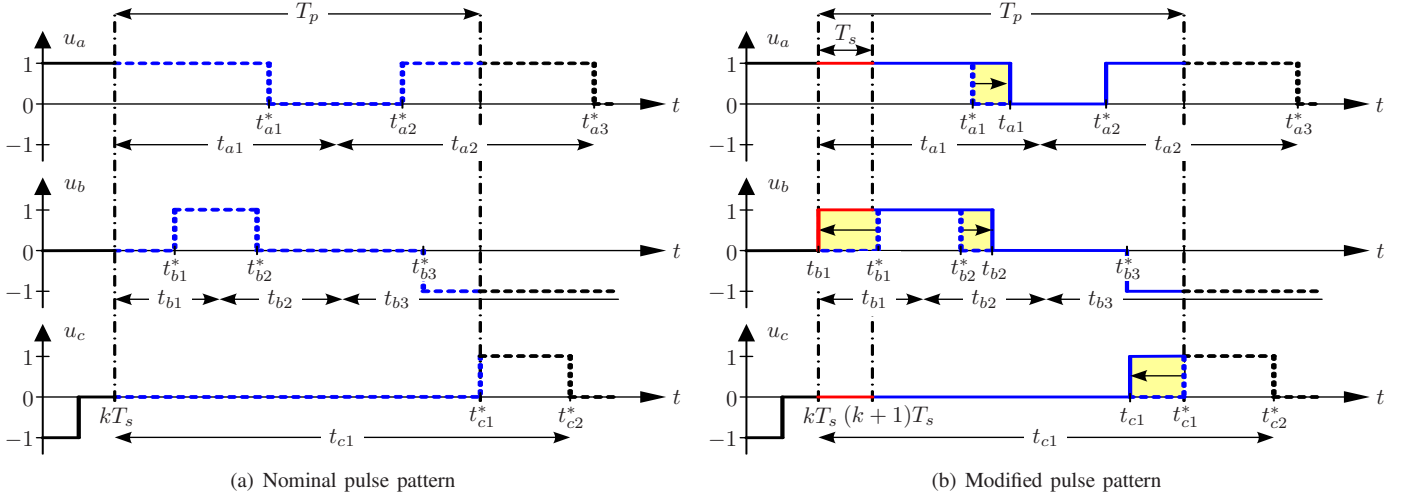


Fig. 4: Three-phase three-level pulse pattern with the nominal switching instants t_x^* and the modified switching instants t_x , where $x \in \{a, b, c\}$. Six switching instants fall within the prediction horizon T_p . The lower and upper constraints on the switching instants are depicted by arrows

switching frequency (or pulse number). Assuming a load with a predominantly inductive characteristic, the current distortions are proportional to the sum of the squared differential-mode voltage harmonics divided by their harmonic order, see [5], [18] and [8, Sect. 3.4].

The integration of the step-wise stator voltage sequence of the OPP over time results in the reference trajectory of the stator flux vector. An example for the latter is shown in Fig. 2.

B. Outer Control Loops

The block diagram of the outer control loops is shown in Fig. 3. Based on the three-phase switch position \mathbf{u}_{abc} and the upper and lower dc-link voltages, the stator voltage $\mathbf{v}_{s,\alpha\beta}$ in stationary orthogonal coordinates is constructed. Based on the latter and the measured stator current vector $\mathbf{i}_{s,\alpha\beta}$, the flux observer estimates the stator and the rotor flux vectors $\psi_{s,\alpha\beta}$ and $\psi_{r,\alpha\beta}$, respectively. The estimate of the electromagnetic torque T_e follows directly.

The speed controller regulates the (electrical) angular speed ω_r of the rotor along its reference ω_r^* by manipulating the set-point of the electromagnetic torque T_e^* . The torque controller manipulates the desired load angle γ^* , i.e. the reference angle between the stator and rotor flux vectors. The torque controller requires the reference of the stator flux magnitude Ψ_s^* and the actual magnitude of the rotor flux vector $\|\psi_{r,\alpha\beta}\|$.

Based on the (instantaneous) dc-link voltage v_{dc} and the angular stator frequency ω_s , the OPP selector sets the modulation index m , such that the magnitude of the stator flux vector remains close to its reference Ψ_s^* . Depending on the fundamental frequency and the maximal allowed switching frequency, the OPP selector also sets the pulse number d .

C. Deadbeat Pulse Pattern Control

By shifting the switching instants of the OPP forward or backward in time, volt-second can be added or removed in each phase. With this principle, the difference between the

reference and the estimated stator flux vectors, i.e. the stator flux error $\psi_{s,\alpha\beta}^*$, can be controlled to zero with the aim to track the ideal stator flux trajectory [8, Chap. 12]. This is typically done in stationary orthogonal $\alpha\beta$ coordinates, as shown in Fig. 2.

During steady-state operation, an accurate tracking of the flux reference trajectory rejects disturbances, such as fluctuations in the dc-link voltage, unmodeled resistive voltage drops and dead-time effects in the inverter. During torque steps, the angular position of the stator flux reference vector changes in a step-wise manner. By correcting the corresponding large stator flux error to zero, the torque is regulated to its new setpoint.

To this end, a model predictive controller is designed, which operates at regularly-spaced sampling instants kT_s , where $k \in \mathbb{N}$ and T_s is the sampling interval. We define the variable-length prediction horizon T_p as the minimum time interval between the current time instant kT_s and a future point in time, such that this time interval includes at least one switching transition per phase. An example is provided in Fig. 4(a), which shows the nominal pulse pattern with dotted lines.

Linear timing constraints on the switching instants are imposed separately per phase to avoid the emergence of non-admissible switch positions (such as $u_x = \pm 2$). If the stator flux error is large, which indicates a torque reference step, additional switching transitions can be inserted in the three phases to fully utilize the available dc-link voltage. This avoids an initial delay in the torque response and minimizes the torque settling time [7].

The stator flux error is translated from stationary orthogonal coordinates into a required three-phase volt-second modification. In each phase, the required volt-second modification is mapped into switching instant modifications of the switching transitions within the prediction horizon. Adopting a deadbeat control principle, the volt-second modification is mapped into the first switching transition, which is then constrained by the timing constraints. Any remaining volt-second modification is



Fig. 5: NPC converter system with an active front end, the terminal and control unit, the inverter unit, the dc-link capacitor bank, a voltage limiter and the water cooling unit

mapped onto subsequent switching transitions. This is shown in phase b in Fig. 4(b), which depicts the modified pulse pattern by solid lines.

Alternatively, an optimization problem with a quadratic cost function and linear constraints, a so-called *quadratic program* (QP), can be defined over a fixed-length prediction horizon. The QP can be solved easily using an active set [6] or a gradient method [19].

Only the first part of the modified pulse pattern, i.e. the switching transitions that fall within the current sampling interval from kT_s to $(k+1)T_s$, are applied to the inverter. In Fig. 4(b), phase b is switched from 0 to 1 at time instant kT_s . At the next sampling instant, a new stator flux estimate and reference are obtained, the prediction horizon is shifted, and the predictions are revised by re-solving the model predictive control problem. This so-called receding horizon policy [9] provides feedback and a high degree of robustness to measurement noise and model errors.

D. Low-Speed Operation

The applicability of OPPs is limited to relatively low pulse numbers, say below 20, owing to limited controller memory and diminishing harmonic benefits over CB-PWM. To extend MP³C to high pulse numbers and thus to low-speed operation, suitable CB-PWM switching patterns with the carrier frequency $f_c = 1/T_c$ are generated online over multiple modulation cycles. The pulse pattern controller regulates the stator flux vector along a circular trajectory by manipulating the switching instants of these online-generated CB-PWM pulse patterns. We refer to this method as carrier-based MP³C [12].

Carrier-based MP³C extends the OPP-based MP³C control methodology to all operating points of a drive system, from operation at standstill to high-speed operation with pulse number one. The switching between OPPs and CB-PWM-generated switching patterns is handled seamlessly by MP³C, similar to a transition between two OPPs with different pulse numbers. In particular, switching between two different control

loops and the initialization of the integrator states of PI controllers are avoided.

E. Balancing of the Neutral Point Potential

The addition of a dc component to the PWM waveform is the classic approach to balance the NP potential v_n , see [20]. By modifying the switching instants of the OPP, this approach can be adopted by MP³C. For example, by widening the pulses in the positive halfwave and narrowing the pulses in the negative halfwave, a positive dc component is added.

To this end, the pulse pattern controller in stationary orthogonal $\alpha\beta$ coordinates is extended by the (virtual) common-mode flux to $\alpha\beta 0$ control. The common-mode flux error is set as a function of the desired NP correction and the phase currents at the nominal switching transitions. The addition of such a common-mode flux error injects a dc component into the pulse pattern.

An alternative NP balancing method based on redundant vectors can be used at low power factors and during large transients that require a fast NP balancing action. The short voltage vectors of the NPC inverter come in pairs, which have the same differential-mode voltage, but opposite common-mode voltages. By choosing the appropriate redundant vector, the NP current can be increased or decreased as desired to achieve NP balancing. In its simplest form, a hysteresis controller on the NP potential acts as a post-processing stage to MP³C.

IV. EXPERIMENTAL RESULTS

A. MP³C Implementation

Deadbeat MP³C was implemented on an industrial drive control platform, which consists of a digital signal processor (DSP) and a small field-programmable gate array (FPGA). The outer control loops predominantly run on the DSP, whereas the pulse pattern controller is executed on the FPGA. For the latter, only a few multipliers, several thousand logic gates and around 100 clock cycles are required. The sampling interval is $T_s = 25\mu\text{s}$.

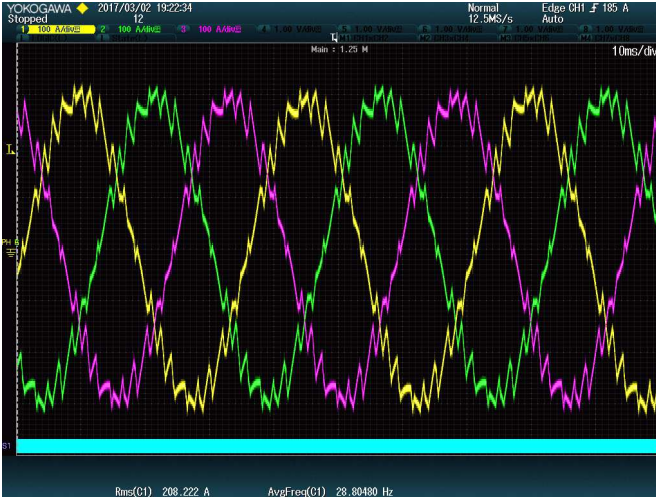


Fig. 6: Experimental results in the MV lab: Steady-state stator currents when operating with MP³C at fundamental frequency 30Hz with pulse number 5

Within this time interval, new measurements are first read in to the DSP and any time delay is compensated for with the help of a converter model. The outputs of the outer control loops are computed next, including the flux observer. The required signals and parameters, see Fig. 3, are then sent to the FPGA, where the inner control loops are run, most notably the pulse pattern controller. Last, the switching signals within the sampling interval are sent to the inverter units, which includes a protection circuit and the gate drivers.

This controller implementation was extensively tested, benchmarked and refined with the help of hardware-in-the-loop (HIL) simulations. More specifically, the industrial drive control hardware with the complete DSP software and FPGA firmware was connected to a HIL system, which emulated the MV drive system in real time. Such a system allows the controller testing for drives with different ratings, machines and configurations.

B. MV Lab Setup

In the MV lab, an NPC inverter is connected with a 3.3kV induction machine rated at 1140kVA. The inverter is complemented on the line side by another NPC converter, an active rectifier unit. Both converters are based on water-cooled integrated-gate-commutated thyristors (IGCTs). The dc-link voltage is set to $v_{dc} = 4.84$ kV. The back-to-back converter system is shown in Fig. 5.

C. Steady-State Operation

Current waveforms are depicted in Fig. 6, showing operation with MP³C at fundamental frequency 30 Hz and at 60% of the rated machine torque. For pulse number 5, the switching frequency is 150 Hz and the total demand distortions (TDD) of the current is 8.7%. Note that the TDD is defined as the harmonic distortions normalized by the rated (rather than the actual) current.

To adhere to the thermal limitations of the converter, the device switching frequency must be kept below the maximal

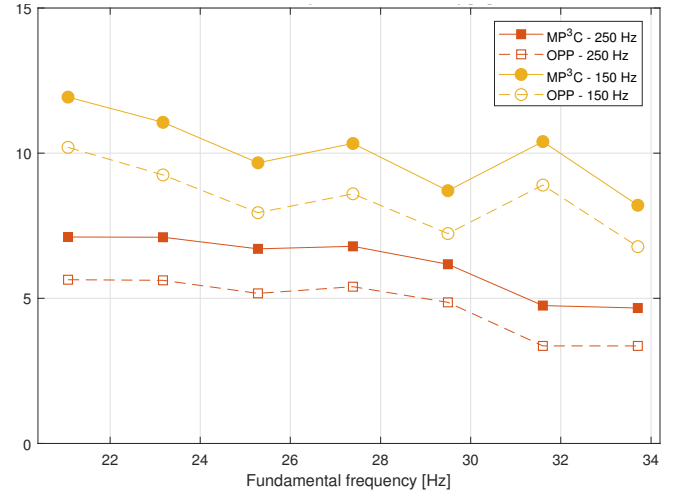


Fig. 7: Experimental results in the MV lab: Measured (solid line) vs theoretical (dashed line) current TDD (in %) at rated torque when varying the fundamental frequency

design switching frequency $f_{sw,max}$. As OPPs are a synchronous PWM method, the pulse number d must be explicitly adjusted when varying the fundamental frequency f_1 . For an NPC inverter, this is done according to $d = \text{floor}(f_{sw,max}/f_1)$.

Fig. 7 depicts the current TDD when operating at seven different fundamental frequencies and at rated torque; the lower solid line relates to the current TDD measurements for MP³C operating at up to $f_{sw,max} = 250$ Hz. The dash-dotted line refers to the theoretical current TDD that results from the OPP. To compute the latter, the harmonic spectrum of the switching function is computed using Fourier analysis. Multiplying their harmonic amplitudes by half the nominal dc-link voltage and scaling the harmonics by their harmonic order and the total leakage inductance, the current spectrum can be computed, from which the theoretical current TDD follows. The difference between the measured and the theoretical TDD is less than 1.85%, both for $f_{sw,max} = 250$ Hz and for $f_{sw,max} = 150$ Hz, see Fig. 7. This difference tends to increase with the torque setpoint, with the figure showing the worst case as it corresponds to operation at rated torque.

The worsening of the current TDD can be attributed to the distinct dc-link voltage ripple, fluctuations in the NP potential, the voltage drop over the stator resistance, deadtimes, as well as minimum on- and off-times that are imposed when operating the semiconductor devices. These imperfections must be compensated for by MP³C. Without such a fast closed-loop controller, the deterioration of the current TDD would be significantly more pronounced. Furthermore, delays are present in the closed-loop control system, the flux observations are noisy and slot harmonics typically exist in MV machines. These attributes lead to a further deterioration of the current TDD. Last, to compute the theoretical current TDD of the nominal OPP, the total leakage inductance of the machine is required. However, this inductance is typically not precisely known, and it changes significantly with the torque. In this experiment, the total leakage inductance was computed based

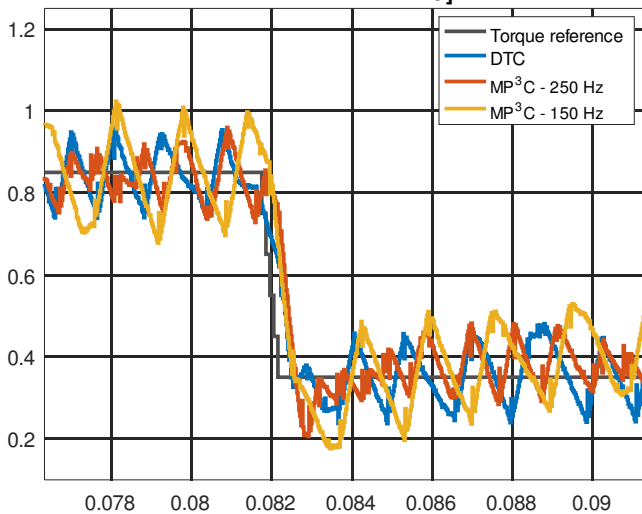


Fig. 8: Experimental results in the MV lab: MP³C and DTC during a torque reference step from 85% to 35% rated torque

on the available machine parameters.

D. Torque Steps

Torque steps from 85% to 35% rated torque are shown in Fig. 8. Thanks to pulse insertion, MP³C achieves the same torque settling time as DTC, which is below 1 ms. Both control methods operate in this test at a switching frequency of about 250 Hz.

V. CURRENT DISTORTIONS VS SWITCHING FREQUENCY

MP³C achieves a superior harmonic performance during steady-state operation. To quantify the corresponding customer benefits, we compare the harmonic performance of MP³C with that of FOC with SVM. The latter is predominantly used for the control of high-performance MV variable speed drive systems.

Consider an inverter-rated MV induction machine with a total leakage reactance of 0.25 per unit (pu), a rated fundamental frequency of 50 Hz and a rated power of 2 MVA. The induction machine is connected to an NPC inverter and operated at rated torque and nominal speed. This speed operating point corresponds to the modulation index $m = 1.04$ (with $0 \leq m \leq 1.27$). Idealized conditions are assumed, i.e., the dc-link voltage is constant, the NP potential is fixed to zero, the stator flux observations are free of noise, delays are neglected and the machine parameters are precisely known.

Using synchronous modulation, we simulated the variable speed drive system for various switching frequencies and determined the stator current TDD using Fourier analysis. Fig. 9 shows the resulting current TDD versus the average switching frequency per semiconductor device. The individual simulations with MP³C are depicted by diamonds, and the FOC simulations are indicated by squares. These data points are approximated by the trend lines.

To achieve a current TDD of about 5%, SVM requires a switching frequency of at least 350 Hz, whereas MP³C

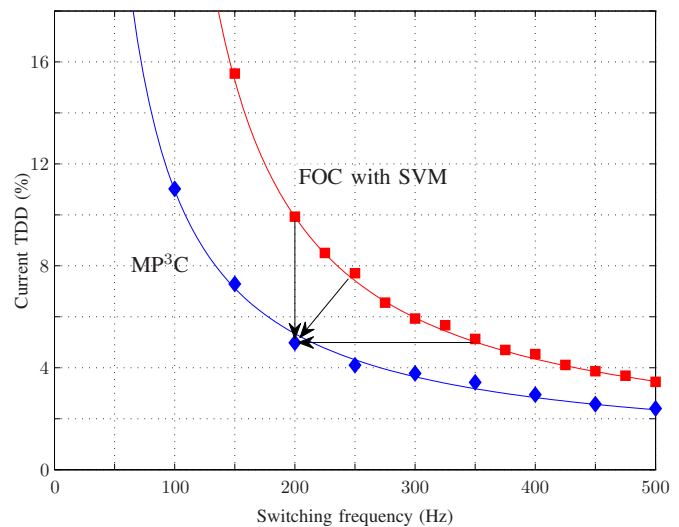


Fig. 9: Simulation results: Stator current TDD as a function of the switching frequency for FOC with SVM and MP³C (operation at nominal speed and rated torque)

requires only 200 Hz, as indicated by the horizontal arrow in Fig. 9. At 5% current distortions, MP³C allows a reduction of the switching frequency by 43% and a similar reduction of the switching losses. Assuming that one third of the semiconductor losses are conduction losses and two thirds are switching losses, this reduces the overall semiconductor losses by almost 30% and increases the overall converter efficiency.

Alternatively, the harmonic current distortions can be reduced. At the switching frequency of 200 Hz, for example, the stator current TDD can be halved from 10% to 5% when using MP³C instead of SVM, see the vertical arrow in Fig. 9. Minimizing the current distortions reduces the iron and copper losses in the electrical machine, which—in turn—lowers the thermal losses. In addition, low stator current distortions imply low torque distortions, thus reducing the likelihood of problems with the mechanical drive train, such as accelerated wear of the shaft and the excitation of eigenmodes of the shaft and mechanical load.

A third alternative is to reduce the switching frequency *and* the current distortions. An example for this approach is provided by the diagonal arrow in Fig. 9. Here, MP³C reduces the switching frequency by 20% and the current TDD by 35%.

These findings are based on simulation results of an idealized variable speed drive system. In a real setup, the dc-link voltage has a strong ripple, the NP potential needs to be balanced, the flux observations are noisy, communication and computation delays exist, and the machine parameters are known only in an approximate manner. These non-idealities do not affect the switching frequency, but they tend to worsen the harmonic current performance. The MV lab results in Sect. IV indicate that the detrimental increase in the current distortions for MP³C is about 1.8%, i.e., a current TDD of 5% obtained either from a harmonic analysis of the nominal OPP or from an idealized simulation setting increases to about 6.8% in the MV lab when operating at rated torque.

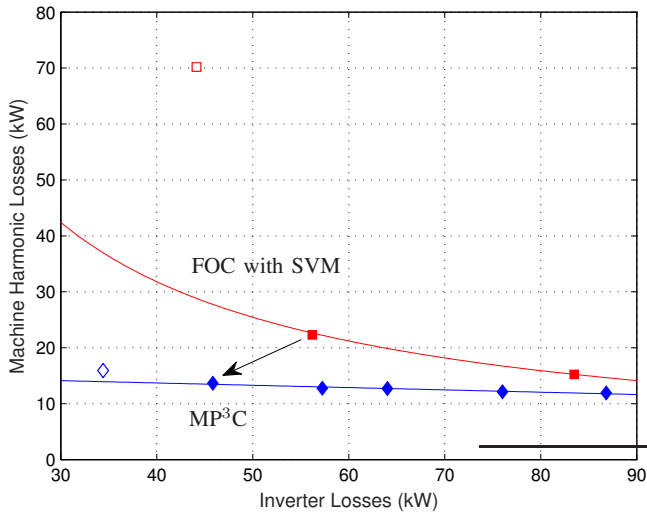


Fig. 10: Simulation results: Trade-off between the harmonic machine losses and the inverter losses

The increase in the current TDD for FOC with SVM is typically even higher, particularly when operating at very low switching frequencies. At 200 Hz switching frequency, for example, the sampling frequency of asymmetric regularly sampled CB-PWM and SVM is with 700 Hz very low, allowing the FOC scheme to control the stator currents only every 1.43 ms. At such a long sampling interval, the disturbance rejection is poor. We conclude that the harmonic benefit of MP³C relative to FOC with SVM equally holds in the MV lab.

VI. CUSTOMER BENEFITS

A fast reaction to disturbances is required in most industrial applications. This is not only true in industries traditionally associated with high dynamics such as metal rolling mills but also in applications where the dynamic requirements might seem much more benign at first glance. In marine propulsion, for example, no fast dynamic requirements are expected from the application (apart from ice going vessels) but the requirement that the drive system remains connected to the network and resumes propulsion after network disturbances implicitly prescribes a significant dynamic capability to the drive control system.

The very small dc-link energy storage in MV applications, with energy stored for typically less than 5 ms, requires a very fast torque reversal during network events to keep the dc-link sufficiently charged. This dynamic performance requirement necessitates the use of a controller with high dynamic performance; with reference to Fig. 1, this has traditionally resulted in either DTC or FOC schemes being used in lieu of OPP-based schemes. MP³C offers a dynamic performance that is comparable to that of DTC. Indeed, in this context, the dynamic performance of MP³C poses a strong sales argument and customer benefit.

Once the appropriate position on the controller bandwidth axis has been determined, the benefits of MP³C in terms of a reduction of the total system losses, as compared to FOC

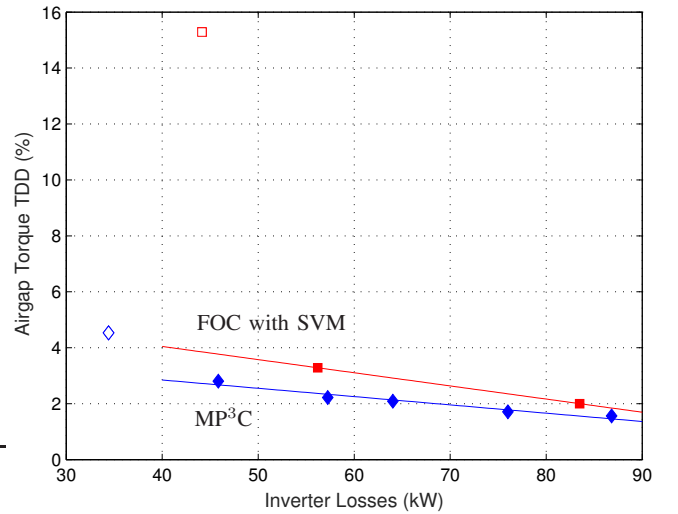


Fig. 11: Simulation results: Trade-off between the torque TDD and the inverter losses

methods for example, can be investigated. The system losses not only determine the operational expenditures of the system in terms of energy costs but they also directly impact the capital costs of the complete system. In the first abstraction layer, the losses in the machine and the inverter unit directly influence the footprint, design complexity, and thus the cost of the inverter unit and machine. In the second abstraction layer, the additional losses that have to be fed from the power grid through the transformer, rectifier unit, cables, and other associated equipment not only drive additional losses in these equipments but also entail size and cost penalties. In the third layer of abstraction, the additional losses must be dealt with in the cooling system, necessitating additional costs in the air-conditioning, ducting, chiller, and related infrastructure.

The operational costs of the system in terms of additional losses in the machine and inverter unit are often significant. Assuming a 98.9% efficiency in the transformer and associated switchgear, a 99.5% efficiency in the rectification process, and a coefficient of performance of 5 in the total cooling system, every 10 kW of losses in the motor and inverter unit entail an additional 12.19 kW at the transformer input. Assuming an electricity price of 80€ per MWh, these 12.19 kW result in an annual bill of 8.5 k€. This cost cannot be neglected, and is often considered during the procurement and design phase.

In an effort to quantify these benefits, detailed simulations of a 3.3 kV drive system with a 10.3 MW induction motor, as detailed in Table I, were carried out. The performance of MP³C at pulse numbers 2–5, 7, and 9 is compared with that of FOC

Voltage	2950 V	R_s	0.0051 pu
Current	2363 A	R_r	0.0061 pu
Real power	10.35 MW	X_{ls}	0.1967 pu
Apparent power	12.07 MVA	X_{lr}	0.1103 pu
Frequency	52.9 Hz	X_m	4.5646 pu
Rotational speed	630.5 rpm		

TABLE I: Rated values (left) and parameters (right) of the machine

using SVM with the carrier multiples 3, 9, and 15. Detailed loss calculations of both the inverter unit and the machine were carried out to determine their harmonic losses. Specifically, in the inverter unit, the (conduction and switching) losses of the semiconductor, the losses in the di/dt clamp circuit, and the resistive losses of the EMC-filter damping resistor were considered. These losses comprise 80–90% of the total inverter losses at typical operating conditions. Equivalently, the harmonic losses of the machine were considered. These losses are defined as the total losses of the machine when operated with the drive using the modulation method of interest minus the total losses when operated at the same operating point with a purely sinusoidal supply. All comparisons were made at full nominal load.

In Fig. 10, the trade-off between the inverter losses and the harmonic losses of the machine is shown when varying the switching frequency. For both MP³C (diamonds) and FOC (squares), a regression line is included to guide the reader (the non-solid data points were considered outliers and ignored in the regression calculation). It is clear from the results that MP³C achieves a superior trade-off in terms of losses. As indicated by the arrow in Fig. 10, MP³C with pulse number 3 achieves a total loss reduction of 25 kW with respect to SVM with the carrier ratio 9. As discussed earlier, this loss reduction can have a significant impact on both the capital as well as the operating costs of the system.

Furthermore, lower stator current distortions imply lower torque distortions. By using MP³C instead of FOC with SVM, the airgap torque TDD can be reduced for similar inverter losses. As shown in Fig. 11, compared with SVM with the carrier ratio 9, MP³C with pulse number 4 reduces the torque TDD from 3.3% to 2.2%, i.e., by 33%. Because of lower mechanical and thermal stress, the lifetime of the electrical machines—and consequently the maintenance intervals—can be extended. This reduces the operating expenditures.

Thanks to its low harmonic distortions at low pulse numbers, MP³C offers the possibility to increase the fundamental frequency. This increases the system design space for applications such as compressors, which require high-speed motors. By increasing the output speed of the drive, the ratio of an additional gearbox can be decreased, leading to a significant cost saving in terms of initial investment.

VII. CONCLUSIONS

This paper proposed a deadbeat MP³C framework for NPC inverters driving MV induction machines. Experimental results for a 3.3 kV induction machine rated at 1140 kVA confirm that MP³C combines the dynamic performance of direct torque control with the superb steady-state harmonic performance of optimized pulse patterns. Compared to SVM, the current distortions can be reduced by up to 50% when operating at the same switching frequency.

With respect to traditional SVM, the customer benefits of MP³C are threefold: (i) lower capital expenditure because of lower initial investment costs, (ii) possibility to optimize the drive train (drive, motor and optional gearbox), and (iii) lower

operational expenditure because of lower running costs. These are achieved by an increased efficiency and lower maintenance costs owing to reduced thermal and mechanical stress on the machine.

ACKNOWLEDGMENTS

The authors would like to thank Henrik Grop from the ABB motor factory in Västerås, Sweden, for his help with the detailed motor loss calculations.

REFERENCES

- [1] B. Wu and M. Narimani, *High-power converters and AC drives*. Wiley, 2nd ed., 2017.
- [2] I. Takahashi and T. Noguchi, “A new quick response and high efficiency control strategy for the induction motor,” *IEEE Trans. Ind. Appl.*, vol. 22, pp. 820–827, Sep./Oct. 1986.
- [3] K. Hasse, “Zum dynamischen Verhalten der Asynchronmaschine bei Betrieb mit variabler Ständerfrequenz und Ständerspannung,” *ETZ-A*, vol. 89, pp. 387–391, 1968.
- [4] F. Blaschke, “Das Prinzip der Feldorientierung, die Grundlage für die Transvector-Regelung von Drehfeldmaschinen,” *Siemens Zeitschrift*, vol. 45, pp. 757–760, 1971.
- [5] G. S. Buja, “Optimum output waveforms in PWM inverters,” *IEEE Trans. Ind. Appl.*, vol. 16, pp. 830–836, Nov./Dec. 1980.
- [6] T. Geyer, N. Oikonomou, G. Papafotiou, and F. Kieferndorf, “Model predictive pulse pattern control,” *IEEE Trans. Ind. Appl.*, vol. 48, pp. 663–676, Mar./Apr. 2012.
- [7] T. Geyer and N. Oikonomou, “Model predictive pulse pattern control with very fast transient responses,” in *Proc. IEEE Energy Convers. Congr. Expo.*, (Pittsburgh, PA, USA), Sep. 2014.
- [8] T. Geyer, *Model predictive control of high power converters and industrial drives*. London, UK: Wiley, Oct. 2016.
- [9] D. Q. Mayne, J. B. Rawlings, C. V. Rao, and P. O. M. Scalet, “Constrained model predictive control: Stability and optimality,” *Automatica*, vol. 36, pp. 789–814, Jun. 2000.
- [10] J. Holtz and B. Beyer, “The trajectory tracking approach—A new method for minimum distortion PWM in dynamic high-power drives,” *IEEE Trans. Ind. Appl.*, vol. 30, pp. 1048–1057, Jul./Aug. 1994.
- [11] J. Holtz and N. Oikonomou, “Synchronous optimal pulsewidth modulation and stator flux trajectory control for medium-voltage drives,” *IEEE Trans. Ind. Appl.*, vol. 43, pp. 600–608, Mar./Apr. 2007.
- [12] T. Geyer and V. Spudic, “Carrier-based model predictive pulse pattern control,” in *Proc. IEEE Energy Convers. Congr. Expo.*, (Portland, OR, USA), Sep. 2018.
- [13] V. Spudic and T. Geyer, “Fast control of a modular multilevel converter STATCOM using optimized pulse patterns,” in *Proc. IEEE Energy Convers. Congr. Expo.*, (Cincinnati, OH, USA), Oct. 2017.
- [14] M. Vasiladiotis, A. Christe, T. Geyer, and A. Faulstich, “Decoupled modulation concept for three-to-single-phase direct AC/AC modular multilevel converters for railway inerties,” in *Proc. Eur. Power Electron. Conf.*, (Warsaw, Poland), Sep. 2017.
- [15] N. Oikonomou, C. Gutscher, P. Karamanakos, F. Kieferndorf, and T. Geyer, “Model predictive pulse pattern control for the five-level active neutral-point-clamped inverter,” *IEEE Trans. Ind. Appl.*, vol. 49, pp. 2583–2592, Dec. 2013.
- [16] P. Al Hokayem, T. Geyer, and N. Oikonomou, “Active damping for model predictive pulse pattern control,” in *Proc. IEEE Energy Convers. Congr. Expo.*, (Pittsburgh, PA, USA), pp. 1220–1227, Sep. 2014.
- [17] T. Geyer, N. Oikonomou, G. Papafotiou, and F. Kieferndorf, “Model predictive pulse pattern control,” in *Proc. IEEE Energy Convers. Congr. Expo.*, (Phoenix, AZ, USA), pp. 3306–3313, Sep. 2011.
- [18] A. K. Rathore, J. Holtz, and T. Boller, “Generalized optimal pulsewidth modulation of multilevel inverters for low-switching-frequency control of medium-voltage high-power industrial AC drives,” *IEEE Trans. Ind. Electron.*, vol. 60, pp. 4215–4224, Oct. 2013.
- [19] S. Richter, T. Geyer, and M. Morari, “Resource-efficient gradient methods for model predictive pulse pattern control on an FPGA,” *IEEE Trans. Contr. Syst. Technol.*, vol. 25, pp. 828–841, May 2017.
- [20] J. K. Steinke, “Switching frequency optimal PWM control of a three-level inverter,” *IEEE Trans. Power Electron.*, vol. 7, pp. 487–496, Jul. 1992.